scatter. (2) Helium-filled tubes are often used to reduce absorption by air in the input or output beam directions. However, as the main problem is generally one of peak-to-background ratio, these measures only slightly affect this ratio, and in any case do not reduce background intensity significantly. It would seem highly advantageous to fill the 'visible volume' with helium, so affecting the background intensity directly. This is obviously difficult to do as it implies either a helium-filled enclosure over the entire diffractometer, or a helium-filled chamber mounted around the φ axis which surrounds the capillary and crystal completely. There are obvious mechanical difficulties in building such a device. First, it must be almost X-ray transparent over the angular ranges used. Second, it must be moderately well sealed to minimize leakage of helium if it encloses the φ drive shaft bearing. A mylar cylinder with solid supports mounted onto the top of the goniometer head would seem to be a good compromise allowing for rigid support of the top and bottom in the X-ray shadow.

(3) Any means of restricting the visible volume will reduce the background in almost direct proportion to the volume change. This can be achieved by placing the final restricting aperture and the scatter cap on the input collimator as close to the crystal as possible. Similarly, there should be a defining aperture as close to the crystal as possible in the crystal–counter pathway, and a second one close to the counter.

We thank Drs A. Kossiakoff and R. Swanson for generously supplying background data, Mr R. Almassy for helpful assistance, and Dr R. E. Marsh and Mr J. Greif for valuable discussions. We are grateful to Dr Sten Samson for allowing us to collect data on diffractometer *F*, a machine designed in the most part by himself, and for his supervision in the redesign of diffractometer *B*. We also recognize his constant attention in the redesign and improvements made to diffractometer *C*.

References

ABRAHAMS, S. C. & KEVE, E. T. (1971). *Acta Cryst.* A**27**, 157–165.
DICKERSON, R. E., KOPKA, M. L., VARNUM, J. & WEINZIERL, J. E. (1967). *Acta Cryst.* **23**, 511–522.
HENDERSON, R. & MOFFATT, J. K. (1971). *Acta Cryst.* B**27**, 1414–1420.
HILL, E. J. & BANASZAK, L. J. (1973). *Acta Cryst.* B**29**, 372.
JENSEN, L. (1972). Personal communication.
KRIEGER, M., KAY, L. M. & STROUD, R. M. (1974). *J. Mol. Biol.* **83**, 209–230.
MATHEWS, F. S., LEVINE, M. & ARGOS, P. (1972). *J. Mol. Biol.* **64**, 449–464.
SALEMME, F. R., FREER, S. T., XUONG, Ng. H., ALDEN, R. & KRAUT, J. (1973). *J. Biol. Chem.* **248**, 3910–3921.
WATSON, H. C., SHOTTON, D. M., COX, J. M. & MUIRHEAD, H. (1970). *Nature, Lond.* **225**, 806–811.
WYCKOFF, H. W., DOSCHER, M., TSERNOGLOU, D., INAGAMI, T., JOHNSON, L. N., HARDMAN, K. D., ALLEWELL, N. M., KELLY, D. M. & RICHARDS, F. M. (1967). *J. Mol. Biol.* **27**, 563–578.
WYCKOFF, H. W., TSERNOGLOU, D., HANSON, A. W., KNOX, J. R., LEE, B. & RICHARDS, F. M. (1970). *J. Biol. Chem.* **245**, 305–328.

Acta Cryst. (1974). A**30**, 748

Highly Anisotropic Extinction

BY F. R. THORNLEY AND R. J. NELMES

Department of Physics, University of Edinburgh, Mayfield Road, Edinburgh EH9 3JZ, Scotland

(*Received* 7 *May* 1974; *accepted* 20 *May* 1974)

An investigation has been made of some large anisotropies observed in the X-ray scattering from a single crystal of Cr–Cl boracite, $Cr_3B_7O_{13}Cl$, in its room-temperature cubic phase. The model of Coppens & Hamilton [*Acta Cryst.* (1970), A**26**, 71–83] for anisotropic secondary extinction has been used to describe the results. Both the type I (domain misorientation) and the type II (domain shape) extinction of that model were found to be present. A new expression for the orientation dependence of type I extinction is introduced, which is believed to be more appropriate to the normal experimental situation. With this modification, the model was able to reproduce fairly well the observed changes in integrated intensity on rotation about the scattering vector. The components of the tensors describing the two types of extinction indicated much greater angular misorientation about the growth axis of the crystal than perpendicular to it, and a domain semi-axis smaller along the growth axis than perpendicular to it.

Introduction

During the collection of X-ray diffraction data for the refinement of the crystal structure of Cr–Cl boracite, $Cr_3B_7O_{13}Cl$, in its room-temperature cubic phase (Nelmes & Thornley, 1974), large differences between the integrated intensities of symmetry-related reflexions were observed. These differences were much too great

to have resulted from absorption, or path-length variation of isotropic extinction. The effects were largest for low-angle strong reflexions. This suggested anisotropies in the extinction properties of the sample, rather than a crystal structure with less than cubic symmetry. This paper describes some further measurements made to investigate the form of the anisotropy and the success of a simple model for secondary extinction in their interpretation.

The theory of extinction in imperfect crystals in current use is that of Zachariasen (1967). This formulation has been extended to allow for angle dependence of the extinction by Cooper & Rouse (1970), and for direction dependence of secondary extinction by Coppens & Hamilton (1970). The model of Coppens & Hamilton (1970) makes detailed predictions of the dependence of the observed integrated intensity on the azimuthal angle of the crystal at the Bragg position. Measurements of the strongest reflexions from Cr–Cl boracite have been made for a number of different azimuthal settings. Large differences in integrated intensity were found, the extinction factor y varying between 0·23 and 0·71 for the strongest reflexion. These results were used to test the predictions of the Coppens & Hamilton model. A small but important modification of this model was found to be necessary.

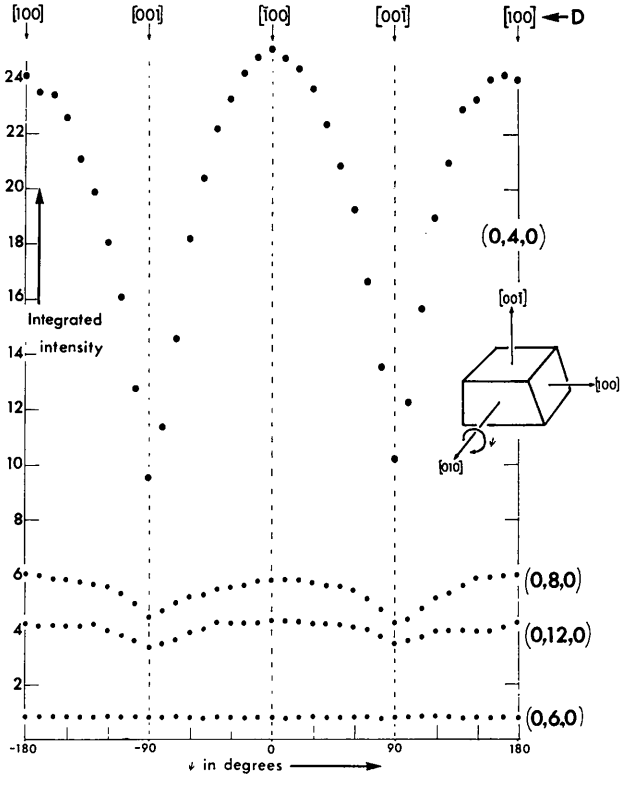

Fig. 1. Variation of integrated intensity with azimuthal angle ψ for $0h0$ reflexions. The intensities have been corrected for absorption and are on an arbitrary scale. The vector **D** indicates the direction which is vertical, *i.e.* perpendicular to the scattering plane.

A more general treatment of the extinction problem has been made recently by Becker & Coppens (1974*a*, *b*). Use of this theory, rather than that of Zachariasen (1967) would not alter the qualitative conclusions. However, there would be major changes in the results for domain size and misorientation obtained from the deduced extinction parameters.

The main intentions of this paper are:

(*a*) To illustrate the large size of the effects which may be produced by anisotropic extinction.

(*b*) To suggest an improved model of anisotropic secondary extinction. A new expression is given for the variation of domain misorientation with direction. This expression gives a much improved fit to the experimental results, and is believed to correspond to the experimental situation more nearly than does that of Coppens & Hamilton (1970).

(*c*) To describe some practical consequences which may be deduced from the form of the new model.

Experimental

Boracites have the general formula $M_3B_7O_{13}X$, where M is a divalent metal and X is Cl, Br or I. For a review of structural and other work on boracites, see Nelmes (1974). Cr–Cl boracite is cubic at room temperature (Schmid, 1965). The crystal structure of the cubic phase was determined by Ito, Morimoto & Sadanaga (1951), and Cr–Cl boracite has been found to have the same structure (Nelmes & Thornley, 1974). The space group is $F\bar{4}3c$, with eight formula units in a cell of side $a = 12{\cdot}132 \pm 0{\cdot}003$ Å.

Crystals of boracites may be grown by vapour transport from a mixture of oxides and the appropriate metal halide in a sealed quartz tube, as described by Schmid (1965). Single crystals of boracites grown in this way frequently show sector growth structure (Schmid, 1969). Different but contiguous parts of the crystal have formed from separate growth centres, and grown along different crystallographic directions, generally of the types ⟨100⟩, ⟨110⟩ or ⟨111⟩. The growth sectors may differ in physical properties such as colour and birefringence. (Some boracites are birefringent even in the cubic phase. This optical anisotropy generally decreases in the sequence I, Br, Cl: for a given halogen it is smallest in the ⟨100⟩ sector.) Our crystal of Cr–Cl boracite was kindly provided by Dr H. Schmid of the Battelle Institute, Geneva. It consisted of a single [100] growth sector, and was a needle of rectangular cross section, dimensions 0·08 × 0·10 mm, length 1 mm. The needle axis was chosen to be [100]; the axes [010] and [001] were perpendicular to the side faces of the needle. For data collection, two samples each of length 0·15 mm were cut from the needle. One of these crystals was used for the present experiment.

The crystal was mounted on a Hilger and Watts four-circle diffractometer, and the [010] direction set parallel to the φ axis. The azimuthal orientation ψ of $(0h0)$ planes may then be changed by changing φ.

Measurements were made of the integrated intensities of a number of $0h0$ reflexions at 10° intervals of φ. Unfiltered Mo $K\alpha$ radiation was used. The results, corrected for absorption (Stewart, 1972), are shown in Fig. 1. The intensity variation is greatest for the strongest reflexion (040). For this reflexion, the ratio of the largest to smallest extimate of the intensity is 2·6. This variation is much greater than could be produced by path-length variation of isotropic extinction.* Smaller effects were found for 080 and 0,12,0; for 060 no systematic change was detected. The observed intensity pattern repeated every 180° and showed a maximum when [100] (the needle axis) was vertical, a minimum when [001] was vertical.

Further measurements of $\{h00\}$ reflexions were made, remounting the crystal and setting [001] and then [100] parallel to the φ axis. The results for {400} reflexions are shown in Fig. 2. For 004, the results were similar to those for 040, the intensity being a maximum when the needle axis was vertical. For 400 there was only about 12% change in intensity as ψ was varied.

A small number of observations were made of {440} and {444} reflexions, with azimuthal settings for which a simple zone axis was vertical. The results were used to confirm the form of the extinction suggested by the $\{h00\}$ reflexions. The integrated intensities of a number of weaker reflexions were also measured. These values were needed for the determination of a scale factor for the principal measurements.

Interpretation

(a) *Model*

The objective is to obtain for each reflexion an expression for the extinction factor y, the ratio of the observed integrated intensity to the kinematical approximation to that intensity. This extinction factor will depend upon the strength of the reflexion, the shape of the crystal, and its extinction properties. The integrated intensity per unit volume of a non-absorbing crystal in the kinematical approximation is equal to $Q=Q_0K$, where K is a polarization factor, and

$$Q_0=|F(hkl)|^2\frac{\lambda^3 L}{V_c^2}. \qquad (1)$$

In (1), $F(hkl)$ is the structure factor in units of scattering length per unit cell, V_c is the volume of the unit cell and L is the Lorentz factor. For normal-beam equatorial geometry, $L=1/\sin 2\theta$. The polarization factor K has average value $K=p_1=\frac{1}{2}(1+\cos^2 2\theta)$ for unpolarized incident X-rays.

The model of an imperfect crystal used by Zachariasen (1967) is an assembly of misoriented perfect spherical domains, with mean radius r. The probability distribution for the angular deviation Δ from the mean orientation of these domains is assumed to be a Gaussian:

$$P(\Delta)=\sqrt{2}g\exp(-2\pi g^2\Delta^2) \qquad (2)$$

with variance $\sigma^2=1/4\pi g^2$. The state of imperfection of the crystal is summarized in the two parameters r and g.

Zachariasen makes a number of physical and mathematical assumptions in his theory; these have been summarized by Coppens & Hamilton (1970). If primary extinction may be neglected, the final expression for the secondary extinction correction y is

$$y=(1+g^*\xi\bar{T})^{-1/2} \qquad (3)$$

where

$$g^*=(\lambda^2/r^2+1/g^2)^{-1/2} \qquad (4)$$

and

$$\xi=\frac{2p_2}{p_1}Q_0, \quad p_n=\frac{(1+\cos^{2n}2\theta)}{2}.$$

The incident radiation is assumed to be unpolarized: the factor p_2/p_1 gives an approximate average over the polarization states of the scattered X-rays. $\bar{T}$ is the absorption-weighted mean path length through the crystal. Thus, in (3), ξ describes the strength of the reflexion, $\bar{T}$ the size and shape of the crystal, and g^* its extinction properties.

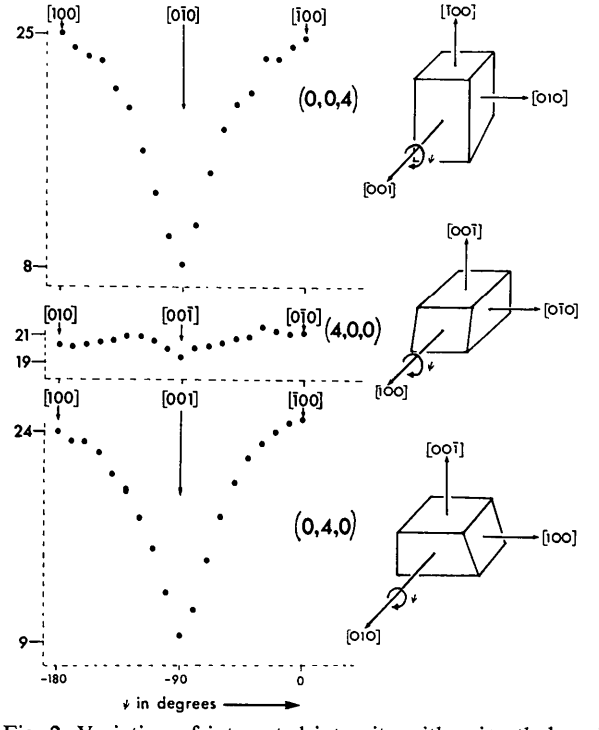

Fig. 2. Variation of integrated intensity with azimuthal angle ψ for {400} reflexions. The intensities have been corrected for absorption and are on the same scale as Fig. 1. For each reflexion, the positions where a cube axis is vertical are indicated.

* The form of the variation is similar to that observed for a plate-shaped crystal rotated about a direction in the plane of the plate: see Arndt & Willis (1966), p. 249.

Zachariasen defines two extreme types of imperfect crystal. The half-width of the diffraction pattern from a single domain is proportional to λ/r. For a type I crystal, $r/\lambda \gg g$, hence $g^* \simeq g$. The intrinsic width of the reflexion, and therefore the amount of extinction, is dominated by the domain misorientation. For a type II crystal, $r/\lambda \ll g$, hence $g^* \simeq r/\lambda$. The intrinsic width of the reflexion, and again therefore the extinction, is dominated by the diffraction width for reflexion from a single domain. Real crystals may lie between these two extremes.

The treatment of Coppens & Hamilton (1970) allows the quantities r and g in (4) to vary with crystal orientation. The domain shape is now assumed to be ellipsoidal, described by a second-rank tensor **W**. If the eigenvalues of **W** are ω_i, $i=1,2,3$, and the half lengths of the corresponding principal axes of the domains are r_i, then $r_i = 1/\sqrt{\omega_i}$. The quantity r in (4) becomes

$$r(\mathbf{N}) = (\mathbf{N}'\mathbf{W}\mathbf{N})^{-1/2} . \quad (5)$$

The unit vector **N** is in the plane of diffraction, and perpendicular to the incident beam.

To allow the probability distribution for angular misorientation of these domains to vary with crystal setting, a second-rank tensor **Z** is introduced, and the function (2) becomes

$$P(\Delta, \mathbf{D}) = \sqrt{2}g(\mathbf{D}) \exp -[2\pi(\mathbf{D}'\mathbf{Z}\mathbf{D})\Delta^2] \quad (6)$$

where the single parameter g is replaced by

$$g(\mathbf{D}) = (\mathbf{D}'\mathbf{Z}\mathbf{D})^{1/2} . \quad (7)$$

The unit vector **D** is perpendicular to the diffraction plane: in the present experiment it is therefore vertical. If the eigenvalues of **Z** are ζ_i, $i=1,2,3$, then the corresponding principal variances of the angular distribution function are $\sigma_i^2 = 1/4\pi\zeta_i$.

Thus the expression describing anisotropic extinction which corresponds to (4) is

$$g^* = \left[\lambda^2 \mathbf{N}'\mathbf{W}\mathbf{N} + \frac{1}{\mathbf{D}'\mathbf{Z}\mathbf{D}}\right]^{1/2} . \quad (8)$$

To describe the extinction properties of a crystal, it is necessary therefore to determine the components of the symmetric tensors **W** and **Z**, referred to some set of axes in the crystal. (Since these tensors reflect, in some way, the growth and subsequent history of the sample, their symmetries have no required relationship to the point symmetry of the crystal. They may be either higher or lower symmetries: for example, higher for a non-cubic crystal with isotropic extinction, lower for a cubic crystal with anisotropic extinction, as here.) In any experimental situation the vectors **N** and **D** are known relative to the same set of axes; hence the expected value of g^* may be calculated. As for isotropic extinction, there are two extreme situations, type I in which $g^* \simeq g(\mathbf{D})$, and type II in which $g^* \simeq r(\mathbf{N})/\lambda$. The terms type I and type II will be used to describe these different kinds of anisotropic extinction, present in the same crystal.

(b) Fitting to results

The experimental results showed how the integrated intensities of sets of symmetry-related reflexions varied with azimuthal angle ψ, *i.e.* with rotation about the scattering vector. Type I extinction depends upon the direction of **D**, which is perpendicular to the scattering vector. Type II extinction depends upon the direction of **N**; for small Bragg angles, this is approximately parallel to the scattering vector.

For analysis of these data, it is convenient to define

$$\mathbf{V} = \lambda^2 \mathbf{W} \quad (9)$$

since only one wavelength was used, and also

$$U = \frac{1}{g^{*2}} = \mathbf{N}'\mathbf{V}\mathbf{N} + \frac{1}{\mathbf{D}'\mathbf{Z}\mathbf{D}} . \quad (10)$$

Since Cr–Cl boracite has cubic symmetry at room temperature, the quantities in (10) may conveniently be referred to the crystal axes x_i, $i=1,2,3$. Let n_i and d_i be the components of the vectors **N** and **D** respectively. Then, for a given reflexion and azimuthal orientation ψ, the form of U may be written down by inspection. Consider for example $0k0$ reflexions, where

$$\begin{aligned} U &= V_{22} + (d_1^2 Z_{11} + 2d_1 d_3 Z_{13} + d_3^2 Z_{33})^{-1} \\ &= V_{22} + (Z_{11}\cos^2\psi + Z_{13}\sin 2\psi + Z_{33}\sin^2\psi)^{-1} \end{aligned} \quad (11)$$

with ψ chosen as 0 when **D** is parallel to [100]. In (11) it is assumed that **N** is parallel to the scattering vector. This is quite a good approximation for the strongest reflexions observed. With Mo $K\alpha$ radiation, the Bragg angles are $\theta = 6{\cdot}7°$ for {400}, 9·5° for {440} and 11·7° for {444}.

Thus each reflexion in Fig. 2 shows principally the effect of variation of type I extinction, described by **Z**, with, in this approximation, no change in type II, described by **V**. The intensity values for {400} reflexions for each position where **D** is parallel to a cube axis are shown in Table 1. The effective components of **Z** and **V** for each measurement are also given, in the same approximation as above – that **N** is parallel to the scattering vector. It is not possible to make a continuous variation in type II extinction alone. However, comparison of different {400} reflexions at positions with the same **D** indicates difference in type II. It isevident that there is considerable anisotropy in type I (results for 040 and 004) and in type II (400 and 004 with **D** parallel to [010]). A model incorporating both types will therefore be necessary.

Type I

The results shown in Fig. 1 have maxima when **D** is parallel to $[\pm 1,0,0]$, and minima when **D** is parallel to $[0,0,\pm 1]$. They are approximately symmetric about these positions. This indicates that the cross term Z_{13} in (11) must be close to zero. From the large change in intensity for 040, $Z_{33} \gg Z_{11}$ (larger Z corresponding to more extinction). The results for 004 in Fig. 2 similarly show $Z_{12} \simeq 0$ and $Z_{22} \gg Z_{11}$. The intensity changes for 400 are rather irregular, but suggest

similar values for Z_{22} and Z_{33}, and hence $Z_{23} \simeq 0$. The principal axes may therefore be chosen to coincide with the crystal axes.

Type II

It is necessary to compare the observed intensities of {400} reflexions for the same **D** and different **N**. The results in Fig. 2 and Table 1 suggest $V_{22} \simeq V_{33} \ll V_{11}$ (smaller V corresponding to more extinction). Some further measurements were made to establish whether the other elements of **V** are zero, as for **Z**. The reflexions chosen were {440} and {444}, which are strong and may give simple forms for the quantity U of equation (10). Some of the measured integrated intensities, corrected for absorption, are given for {440} in Table 2.

The explicit forms of **N'VN** and **D'ZD** are also listed. It is assumed that **Z** is diagonal, and that as before **N** is parallel to the scattering vector. Comparison of pairs of reflexions, for which the form of U differs only in the signs of the off-diagonal elements of **V**, suggest that these elements are small. Some of these differences may have resulted from variations in the mean path length. In the remainder of the analysis, it will be assumed that both **Z** and **V** are diagonal when referred to the crystal axes.

(*c*) *Extinction parameters*

To determine the components of the tensors **V** and **Z**, it is necessary to estimate the values of g^* from the observed intensities, using equation (3) for the extinction factor y. The information which is needed is:

(i) the scale factor,

(ii) the expected kinematical intensity per unit volume, Q, for each reflexion: this is required both to obtain a value of y from each observed intensity, and to calculate the factor ξ occurring in (3), and

(ii) the absorption-weighted mean path length $\bar{T}$ for each measurement, also occurring in (3).

For (i) and (ii), use was made of the results of the refinement of the cubic crystal structure of Cr–Cl boracite (Nelmes & Thornley, 1974). The samples used in the data collection and for the present experiment were cut from the same needle-shaped single [100] growth sector, and were of similar dimensions. In the structural study, an orientation for the sample was chosen which minimized the anisotropy of the extinction; an isotropic extinction factor in the least-squares refinement worked well. The conventional R index obtained was 2·5%. The calculated structure factors in the final refinement have been used to estimate the values of Q which are needed for the present experiment. A scale factor was estimated from a comparison of the intensities of some weaker reflexions in the two experiments, reflexions for which extinction effects would be small.

The path lengths $\bar{T}$ may be obtained from the values of the absorption factor A^* calculated for each measurement. The expression used was $\bar{T} = (\ln A^*)/\mu$, where $\mu = 41{\cdot}3$ cm^{-1} is the absorption coefficient of Cr–Cl boracite for Mo $K\alpha$ radiation.

The experimental values of the extinction factor y obtained are given for {400} in Table 1 and for {440}

Table 1. *Principal measurements of* {400} *reflexions*

h	k	l	N'VN	D	D'ZD	Integrated intensity (arbitrary scale)	Extinction factor y	U (10^{-8})
4	0	0	V_{11}	[010]	Z_{22}	2046 (25)	0·584 (7)	1·51 (8)
				[001]	Z_{33}	1919 (24)	0·547 (7)	1·45 (10)
0	4	0	V_{22}	[100]	Z_{11}	2416 (28)	0·689 (8)	4·4 (4)
				[001]	Z_{33}	987 (17)	0·282 (5)	0·098 (7)
0	0	4	V_{33}	[100]	Z_{11}	2472 (32)	0·706 (9)	7·9 (8)
				[010]	Z_{22}	825 (20)	0·235 (6)	0·044 (5)

Table 2. *Principal measurements of* {440} *reflexions*

h	k	l	N'VN	D	D'ZD	Integrated intensity (arbitrary scale)	Extinction factor y
4	0	4	$\frac{1}{2}(V_{11}+2V_{13}+V_{33})$	[010]	Z_{22}	950 (9)	0·676 (6)
4	0	$\bar{4}$	$\frac{1}{2}(V_{11}-2V_{13}+V_{33})$	[010]	Z_{22}	905 (9)	0·644 (6)
4	4	0	$\frac{1}{2}(V_{11}+2V_{12}+V_{22})$	[$\bar{1}$10]	$\frac{1}{2}(Z_{11}+Z_{22})$	1168 (10)	0·831 (8)
				[001]	Z_{33}	920 (9)	0·655 (6)
$\bar{4}$	4	0	$\frac{1}{2}(V_{11}-2V_{12}+V_{22})$	[110]	$\frac{1}{2}(Z_{11}+Z_{22})$	1137 (10)	0·809 (7)
				[001]	Z_{33}	880 (9)	0·626 (6)
0	4	4	$\frac{1}{2}(V_{22}+2V_{23}+V_{33})$	[01$\bar{1}$]	$\frac{1}{2}(Z_{22}+Z_{33})$	651 (9)	0·463 (6)
				[$\bar{1}$00]	Z_{11}	1200 (10)	0·854 (7)
0	4	$\bar{4}$	$\frac{1}{2}(V_{22}-2V_{23}+V_{33})$	[011]	$\frac{1}{2}(Z_{22}+Z_{33})$	639 (9)	0·455 (6)
				[100]	Z_{11}	1114 (10)	0·793 (7)

in Table 2. For {400}, y varies between 0·23 and 0·71 as the crystal orientation is changed. The values of $U=1/g^{*2}$ are also given in Table 1.

Some deductions may be made from the results in Table 1; the multiplying factor of 10^{-8} for U will be omitted below. From 400,

$$V_{11}+1/Z_{22}\simeq V_{11}+1/Z_{33}=1\cdot5 \qquad (12)$$

and from 040

$$V_{22}+1/Z_{11}=4\cdot4 \qquad (13)$$

$$V_{22}+1/Z_{33}=0\cdot098\,. \qquad (14)$$

Therefore

$$1/Z_{33}<0\cdot098 \qquad (15)$$

and

$$V_{22}<0\cdot098. \qquad (16)$$

Hence

$$V_{11}=1\cdot5, \text{ from (12)}, \qquad (17)$$

and

$$1/Z_{11}=4\cdot4, \text{ from (13)}, \qquad (18a)$$

with the smaller terms neglected.
Similarly, 004 gives

$$1/Z_{22}<0\cdot044 \qquad (19)$$

$$V_{33}<0\cdot044 \qquad (20)$$

and

$$1/Z_{11}=7\cdot9\,, \qquad (18b)$$

somewhat different from (18*a*).

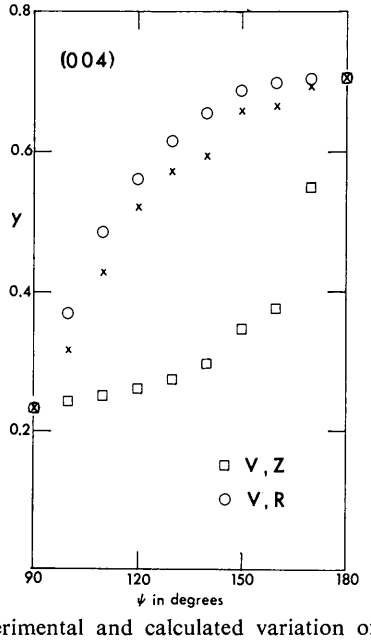

Fig. 3. Experimental and calculated variation of extinction factor y with azimuthal angle ψ for 004 reflexion. The crosses are experimental points. The squares are calculated values using (3) and (10). That is, $U=V_{33}+(Z_{11}\cos^2\psi+Z_{22}\sin^2\psi)^{-1}$ with $V_{33}=1/Z_{22}=0\cdot022\times10^{-8}$, $1/Z_{11}=7\cdot9\times10^{-8}$. The circles are calculated values using (3) and (26). That is, $U=V_{33}+R_{11}\cos^2\psi+R_{22}\sin^2\psi$ with $V_{33}=R_{22}=0\cdot022\times10^{-8}$, $R_{11}=7\cdot9\times10^{-8}$.

For the positions where the extinction is greatest, it is not possible to make this separation of U into contributions from type I and type II extinction.

The corresponding restrictions on the half lengths of the principal axes of the domains described by **V** are

$$r_1=0\cdot58\ (2)\ \mu\text{m}$$
$$r_2>2\cdot3\ (1)\ \mu\text{m}$$
$$r_3>3\cdot4\ (2)\ \mu\text{m}\,.$$

If the principal variances of the angular distribution function represented by **Z** are σ_i^2, then

$$\sigma_1=12\cdot2\ (5)'', \text{ from (18}a\text{)},$$
$$\sigma_1=16\ (1)'', \text{ from (18}b\text{)},$$
$$\sigma_2<1\cdot22\ (7)''$$
$$\sigma_3<1\cdot82\ (7)''\,.$$

The estimated errors include only the counting statistics of the original measurements. There will be additional systematic effects from uncertainties, for example in the structure factor $F(400)$ and the scale factor. However, the principal interest is in the anisotropies and their description.

In an attempt to separate the contributions from type I and type II extinction in, for example, equation (14), calculations were made of the expected intensity at intermediate values of ψ, corresponding to the results shown in Fig. 2. Different proportions of the two types of extinction were tried, but it was not possible to obtain qualitative agreement using parameters fitted to the maximum and minimum values. An example is shown in Fig. 3; the crosses are experimental points for 004, as in Fig. 2, and the squares are calculated values with

$$V_{33}=1/Z_{22}=0\cdot022\times10^{-8} \text{ and } 1/Z_{11}=7\cdot9\times10^{-8}$$

giving a fit to the experimental points at $\psi=90$ and $\psi=180°$, and dividing the extinction at $\psi=90°$ equally between type I and type II extinction. The discrepancy is very marked, the observed intensity increasing with ψ much more rapidly than the calculated values suggest. The degree of anisotropy is much greater than in the examples considered by Coppens & Hamilton (1970).

(*d*) *New model*

Thus the model of anisotropic extinction summarized in (3) and (8) has failed to describe the details of the observed intensity variation. It has been found that with a different description of the type I extinction, a much better fit to the results is obtained. In this section, the new expression is defined, and an account is given of the form of the extinction which it predicts.

The requirement is a function to represent the probability distribution for angular deviation from the mean orientation. This will replace (2), a Gaussian with variance $\sigma^2=1/4\pi g^2$. A simple way of allowing g, and therefore σ, to vary with direction, is to introduce

some second-rank tensor. The probability distribution for angular deviation about each principal axis of this tensor is assumed to be a Gaussian of the form (2). That is

$$P(\Delta_1,\Delta_2,\Delta_3)=2^{3/2}g_1g_2g_3 \times \exp -[2\pi(g_1^2\Delta_1^2+g_2^2\Delta_2^2+g_3^2\Delta_3^2)] \quad (21)$$

for angular deviations Δ_i, $i=1,2,3$, about the principal axes, a trivariate Gaussian with variances $\sigma_i^2=1/4\pi g_i^2$.

What is sought is a probability distribution $P(\Delta,\mathbf{D})$ for angular deviation Δ about some direction defined by a unit vector **D**. In the experiment **D** is, as before, perpendicular to the plane of diffraction. Let **D** have components d_i, $i=1,2,3$, referred now to the principal axes of (21). The angles of misorientation are assumed to be sufficiently small for them to combine as vectors.

Suppose that the crystal has been rotated by $-\Delta$ about **D** away from the mean Bragg position. Two ways of defining $P(\Delta,\mathbf{D})$ have been considered, by estimating the following:

(1) The probability of a domain having such a misorientation that it is now exactly at the Bragg position. That is, the domain has misorientation Δ about **D**. This necessary rotation may be resolved into rotations $d_i\Delta$, $i=1,2,3$ about the principal axes. The probability of these three rotations is

$$P_1(\Delta,\mathbf{D})=\sqrt{2}(g_1^2d_1^2+g_2^2d_2^2+g_3^2d_3^2)^{1/2} \times \exp -[2\pi(g_1^2d_1^2+g_2^2d_2^2+g_3^2d_3^2)\Delta^2)] \quad (22)$$

which is a Gaussian with variance $\sigma^2=(d_1^2/\sigma_1^2+d_2^2/\sigma_2^2+d_3^2/\sigma_3^2)^{-1}$. This is the expression (6) used by Coppens & Hamilton (1970), with $\mathbf{D}'\mathbf{Z}\mathbf{D}=(g_1^2d_1^2+g_2^2d_2^2+g_3^2d_3^2)$, and the eigenvalues of **Z** given by $\zeta_i=g_i^2$.

(2) The probability of a domain having a misorientation about *any* direction, of such a magnitude that it has a component Δ about **D**. This may be obtained by projecting (21) onto the direction **D**. The resulting expression is (Nelmes, 1969)*

$$P_2(\Delta,D)=\sqrt{2}(d_1^2/g_1^2+d_2^2/g_2^2+d_3^2/g_3^2)^{-1/2} \times \exp -[2\pi\Delta^2/(d_1^2/g_1^2+d_2^2/g_2^2+d_3^2/g_3^2)], \quad (23)$$

a Gaussian with variance $\sigma^2=(d_1^2\sigma_1^2+d_2^2\sigma_2^2+d_3^2\sigma_3^2)$. This distribution may be represented by a tensor **R**, where $\mathbf{D}'\mathbf{R}\mathbf{D}=(d_1^2/g_1^2+d_2^2/g_2^2+d_3^2/g_3^2)$. The eigenvalues of **R** are $\varrho_i=1/g_i^2=1/\zeta_i$.

If $g(\mathbf{D})$ is defined by

$$g(\mathbf{D})=(\mathbf{D}'\mathbf{R}\mathbf{D})^{-1/2}, \quad (24)$$

(23) may be written more concisely as

$$P_2(\Delta,\mathbf{D})=\sqrt{2}g(\mathbf{D}) \exp -(2\pi\Delta^2/\mathbf{D}'\mathbf{R}\mathbf{D}). \quad (25)$$

This result (25) may be used as an alternative to (22) for the description of type I extinction. The formalism is as before, with

$$U=1/g^{*2}=\mathbf{N}'\mathbf{V}\mathbf{N}+\mathbf{D}'\mathbf{R}\mathbf{D} \quad (26)$$

replacing (10), and (24) replacing (7). The principal axes of the tensors **Z** and **R** coincide. The expressions (22) and (25) simplify to the same distribution when **D** lies along any one of the principal axes. However, the two expressions may give results different from one another if **D** is in a general direction. What is the physical significance of this difference?

In the experimental situation, the scattered X-rays are detected as the crystal is rotated through the Bragg position. For normal-beam equatorial geometry, the rotation axis is perpendicular to the diffraction plane, *i.e.* parallel to **D**. It is assumed that the collimation of the incident beam is such that all domains pass through the Bragg position as the crystal is rotated. (This is generally true, since the effective angular spread of imperfect crystals is usually a few minutes or, as here, seconds of arc. Indeed, if this is not so, then the integrated intensity from the whole crystal is not being measured.) It follows that the distribution $P_2(\Delta,\mathbf{D})$, equation (25), is the appropriate one. $P_1(\Delta,\mathbf{D})$, equation (6) or (22), corresponds to perfect collimation of the incident beam, a too restrictive condition. Away from the principal axes, where they agree, $P_1(\Delta,\mathbf{D})$ gives a narrower distribution than $P_2(\Delta,\mathbf{D})$, as is suggested by a comparison of the expressions for the variances of the distributions. Thus the extinction will be less and the intensity greater if $P_2(\Delta,\mathbf{D})$ is used. This may be seen in Fig. 3, where the circles show the values calculated from (26), with

$$V_{33}=R_{22}=0{\cdot}022\times10^{-8} \text{ and } R_{11}=7{\cdot}9\times10^{-8}.$$

The calculated intensity values increase with ψ much more rapidly than did the previous calculations (squares). They are much closer to the experimental values; the shape of the intensity variation with azimuth is correct.

The results for {440} reflexions are also in better agreement with the new model. The parameters obtained from the {400} reflexions were used to calculate expected values of y for the {440} reflexions. For most reflexions and orientations, the two models gave results which were similar to each other and in reasonable agreement with the experimental values. However, there were differences between the two models for 440, measured with [$\bar{1}$10] and [001] vertical. For the old model, with tensors **V** and **Z**, the predicted values are similar to each other: $y=0{\cdot}703$ and $y=0{\cdot}649$ respectively. For the new model, the predicted values are $y=0.838$ and $y=0.649$, in good agreement with the experimental values of $y=0{\cdot}831$ (8) and $y=0{\cdot}655$ (6). This quantitative agreement is probably fortuitous, because of uncertainties in the experimental results and the simplicity of the model. However, the qualitative differences are certainly in favour of the new model.

* There is an error in the normalization factor in the appropriate equation (9) of this paper; it should read $[2\pi(u_1^2n_1^2+u_2^2u_2^2+u_3^2n_3^2)]^{-1/2}$.

To illustrate the differences between the two descriptions of type I extinction, calculations have been made of the expected form of the variation of intensity with azimuthal angle ψ for a hypothetical crystal. They have been made for a range of values of the dimensionless quantity $\xi\bar{T}$ in equation (3); this is essentially the product of the kinematical integrated intensity per unit volume and the mean path length through the crystal. A degree of anisotropy was assumed which would give an extinction factor varying between $y=0{\cdot}2$ and $y=0{\cdot}8$ for a strong reflexion with $\xi\bar{T}=3{\cdot}00\times10^{-4}$. (This was the appropriate value of $\xi\bar{T}$ for the strongest reflexion from Cr–Cl boracite with Mo $K\alpha$ radiation and $\bar{T}$ equal to 0·1 mm). For type I extinction alone, the change in intensity corresponds to σ varying between 0·73″ and 31″. The extinction factor has been calculated as a function of ψ for the following values of $\xi\bar{T}$: 3·00, 0·50, 0·10 and 0·01, all $\times10^{-4}$. The results are shown in Fig. 4. To represent type I extinction, the tensor **Z** was used for ψ increasing from 0° to 90°, and the tensor **R** for ψ decreasing from 90° to 0°.

The differences between the two models are quite marked, even for the weaker reflexions. Firstly, as seen in Fig. 3, on moving away from a position where there is considerable extinction, the intensity rises with ψ much more rapidly when **R** is used. Secondly, the **Z** model is more sensitive to the relative proportions of type I and type II extinction. The three (*a*) curves correspond to different proportions, giving the same overall effect at $\psi=0$. When **R** is used the same variation produces differences too small to show. Thirdly, the **R** model concentrates much of the intensity variation with azimuth over a small range of ψ, especially for the weaker reflexions. Consider the curves (*c*) and (*c*′) for $\xi\bar{T}=0{\cdot}10\times10^{-4}$, a fairly weak reflexion for the samples and radiations in common use. (If the structure factor is 0·01 electrons Å^{-3}, for example $F=10$ electrons for a cell $10\times10\times10$ Å, then with Cu $K\alpha$ radiation, with the Lorentz and polarization factors neglected, the value of ξ is about 0·04 m^{-1}. If $\bar{T}=0{\cdot}2$ mm, then $\xi\bar{T}=0{\cdot}08\times10^{-4}$.) Over the range $\psi=90$ to $\psi=10°$, the intensity decreases by 4%; over the range $\psi=10$ to $\psi=0°$, it decreases by a further 20%. For the **Z** model, almost all the 24% decrease occurs within the range $\psi=90$ to $\psi=10°$.

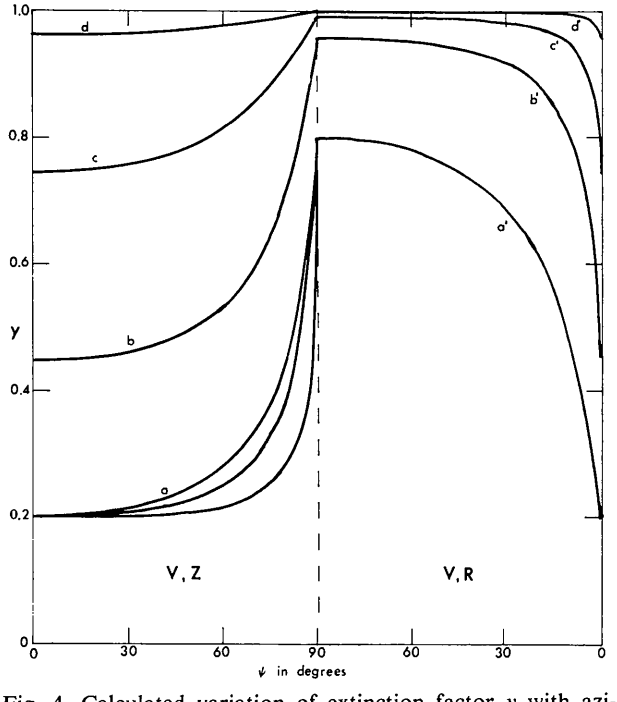

Fig. 4. Calculated variation of extinction factor y with azimuthal angle ψ for a hypothetical crystal. Calculations have been made using (3), with a,a': $\xi\bar{T}=3{\cdot}00\times10^{-4}$; b,b': $\xi\bar{T}=0{\cdot}50\times10^{-4}$; c,c': $\xi\bar{T}=0{\cdot}10\times10^{-4}$; d,d': $\xi\bar{T}=0{\cdot}01\times10^{-4}$. At $\psi=0°$, $U=0{\cdot}0156\times10^{-8}$: at $\psi=90°$, $U=28{\cdot}4\times10^{-8}$. To obtain the curves a,b,c,d, equation (10) was used for U (tensors **V** and **Z**). The different curves *a* correspond to different proportions of type I and type II extinction at $\psi=0°$. To obtain the curves a',b',c',d', equation (26) was used for U (tensors **V** and **R**).

It has been suggested that the new model with the tensor **R** is correct, rather than that with the tensor **Z**. Therefore an intensity variation like (*c*′) would be expected. For most diffractometer experiments, the value of azimuthal angle for each reflexion is a matter of chance, depending upon how the crystal is mounted on the goniometer and upon the diffraction geometry in use. Thus of a group of reflexions with approximately the same kinematic intensity, corresponding to (*c*′) for example, a small fraction may be reduced in intensity appreciably more than the rest. An isotropic extinction correction could not deal with this.

(*e*) *Primary extinction*

It has been assumed that there is only secondary, and no primary extinction. However, the estimated semi-axes of the perfect domains r_i may be as large as several microns, hence the expected magnitude of primary extinction needs to be considered. The expression given by Zachariasen (1967) for the extinction factor y in the presence of primary extinction may be written:

$$y=\{1+\xi[\bar{t}g_p+(\bar{T}-\bar{t})g^*]\}^{-1/2} \qquad (27)$$

where $\bar{t}$ is the mean path length through a perfect domain. For spherical domains of radius r, $\bar{t}=\frac{3}{2}r$ and $g_p=r/\lambda$. This expression simplifies to (3) if $\bar{t}$ is neglected; primary and secondary extinction are equivalent if g is very large, since then $g^*=g_p$.

To extend (25) to allow for ellipsoidal domains, described by the tensor **W**, r in the expression for g_p may be replaced by $r(\mathbf{N})=(\mathbf{N}'\mathbf{W}\mathbf{N})^{-1/2}$, equation (5). Therefore

$$g_p=(\mathbf{N}'\mathbf{V}\mathbf{N})^{-1/2}, \qquad (28)$$

if the definition (9) of **V** is used. This expression for g_p may be compared with (26) for g^*. The mean path length through a domain $\bar{t}$, will also depend upon the orientation of the domain. For small Bragg angles, the

mean path length along the direction of the incident beam may be taken. If **L** is a unit vector parallel to the incident beam, then

$$\bar{t}=\tfrac{3}{2}[\mathbf{L}'\mathbf{W}\mathbf{L}]^{-1/2}. \quad (29)$$

The vectors **L**, **N**, and **D** are mutually perpendicular.

For the Cr–Cl boracite crystal, $\bar{t}$ is expected to be no more than a few microns, and $\bar{T}$ is about 100 microns, hence primary extinction will be small relative to secondary unless g_p is much greater than g^*. From the expression (24) this will occur if g^* is dominated by type I extinction. For {400} reflexions, the main positions when this occurs are 004 and 040 with **D** along [100]. For 040, $V_{22}<0{\cdot}098\times10^{-8}$, hence $g_p>3{\cdot}19\times10^4$. Taking **L** along [001] for simplicity, $\bar{t}=\frac{3}{2}(\lambda/\sqrt{V_{33}})$, where $V_{33}<0{\cdot}044\times10^{-8}$. Hence $\bar{t}>5{\cdot}1$ μm, and $\bar{t}g_p>0{\cdot}16$ m. However, the experimental value in this position of $[\bar{t}g_p+(\bar{T}-\bar{t})g^*]$ is 0·38 (2)m. Thus a considerable error will be introduced into the estimate of $g^*=[V_{22}+R_{11}]^{-1/2}$, and thus into σ_1, if primary extinction is neglected. The other values of r_i and σ_i are not affected significantly, hence the above elements of **V** may be used for the estimate of primary extinction in this position.

However, the qualitative conclusions on the anisotropy of the secondary extinction are not affected. Indeed, allowance for primary extinction in the 004 and 040 reflexions when **D** is along [100] would increase the estimated values of σ_1, possibly removing the discrepancy between the two estimates, and thus indicate even greater anisotropy in type I extinction. It is curious that, because of the shape of the domains, primary extinction is greatest when the observed intensity is greatest.

Discussion

Extinction

The usefulness of any extinction correction is dependent upon agreement with experimental results. The measurements on Cr–Cl boracite indicated the need for a formalism which would allow the magnitude of type I and type II extinction to vary with direction. A new description of anisotropic type I extinction has been given, which is believed to correspond more correctly to the experimental situation. With this change, the model of Coppens & Hamilton (1970) reproduced the broad features of the experimental results, although there were some discrepancies. These may have resulted from errors or inadequacies in the model, in addition to the neglect of primary extinction and double reflexion.

Tests of the results (26) on other crystals would be of interest. Anisotropic extinction should be considered if there are difficulties with an isotropic extinction correction – for example, if the extinction appears to be underestimated for a few reflexions. Coppens & Hamilton (1970) describe how to incorporate the refinement of the elements of the appropriate tensors into the least-squares refinement; or an investigation such as that described here may be made. This indicated that choosing a different orientation of the sample would reduce the effects of the anisotropy (Nelmes & Thornley, 1974).

The expressions for primary and secondary extinction described by Becker & Coppens (1974*a*) differ in important respects from those of Zachariasen (1967). Results were given for isotropic extinction in imperfect spherical crystals. The expressions for primary and secondary extinction, which correspond to (3), include angle-dependent factors. Explicit angle dependence also occurs in the expression corresponding to (4); r is replaced by $l\sin2\theta$, where l is the mean radius of a domain along the diffracted beam. In addition to the Gaussian distribution (2), a Lorentzian distribution was considered.

There would be corresponding differences between the treatment of Coppens & Hamilton (1970), as modified above, and the extension of the results of Becker & Coppens (1974*a*) to anisotropic extinction. The vector **N** in (5) would be replaced by a vector parallel to the diffracted beam, and the factor $\sin2\theta$ introduced into (8) or (26), in addition to alternative forms for Gaussian and Lorentzian distributions. Use of this theory for analysis of the present results alters the interpretation of the type II extinction; the ellipsoidal domains have a semi-axis longer along the needle axis than perpendicular to it. However, it is not possible with the present results to distinguish between Lorentzian and Gaussian distributions for angular misorientation of the domains, or indeed to choose between the two theories. The qualitative arguments on the effect of anisotropic extinction are unaffected.

Boracites

The parameters of the tensors **V** and **R** (or **Z**) indicate:

(1) The principal axes of the tensors describing both type I and type II extinction coincide with the crystal axes.

(2) That semi-axis of the assumed ellipsoidal perfect domains which is parallel to the needle axis (r_1) is smaller than the semi-axes perpendicular to the needle axis.

(3) There is much greater angular misorientation about the needle axis (σ_1) than perpendicular to it.

These relations between **V** and **R**, the crystal axes and the needle axis (presumably the growth direction) suggest that the observed scattering properties do reflect in some way the true arrangement of defects in the crystal. It would be of great interest to investigate the defect structure to see if the crystal does appear more perfect for directions perpendicular to the growth direction than parallel to it. In a boracite the defects are probably mostly grown-in, rather than a result of the subsequent history of the crystal.

The model used is a convenient way of describing

the average effect of these defects over the whole crystal. There will be perfect regions within the crystal, but defects such as dislocations and stacking faults do not normally dissect a crystal into discrete misoriented domains. The term 'ellipsoidal perfect domains' has been used above for convenience, but it should not be imagined that the authors believe in such objects *per se*. The expression (5) is a simple way of allowing the average perfect dimension along **N** to vary with crystal orientation.

It is not known whether the sample of Cr–Cl boracite is exceptional in its defect structure for boracites, or for crystals grown by vapour transport. The form of a needle is, however, very unusual (Schmid, 1973). It is intended to continue with measurements of the kind described here, on boracites and other materials, in combination if possible with study of the defects by X-ray topography.

We should like to thank Dr G. S. Pawley for illuminating discussions and Dr S. E. B. Gould for her help in data reduction. One of us (RJN) gratefully acknowledges the financial support of a Science Research Council Research Fellowship.

References

ARNDT, U. W. & WILLIS, B. T. M. (1966). *Single Crystal Diffractometry*. Cambridge Univ. Press.
BECKER, P. J. & COPPENS, P. (1974*a*). *Acta Cryst.* A**30**, 129–147.
BECKER, P. J. & COPPENS, P. (1974*b*). *Acta Cryst.* A**30**, 148–153.
COOPER, M. J. & ROUSE, K. D. (1970). *Acta Cryst.* A**26**, 214–223.
COPPENS, P. & HAMILTON, W. C. (1970). *Acta Cryst.* A**26**, 71–83.
ITO, T., MORIMOTO, N. & SADANAGA, R. (1951). *Acta Cryst.* **4**, 310–316.
NELMES, R. J. (1969). *Acta Cryst.* A**25**, 523–526.
NELMES, R. J. (1974). *J. Phys. C. Solid State Phys.* **7**, 3840–3854.
NELMES, R. J. & THORNLEY, F. R. (1974). *J. Phys. C. Solid State Phys.* **7**, 3855–3874.
SCHMID, H. (1965). *J. Phys. Chem. Solids* **26**, 973–988.
SCHMID, H. (1969). *Growth Cryst.* **7**, 25–52.
SCHMID, H. (1973). Private communication.
STEWART, J. M. (1972). *The X-RAY System – Version of June* 1972. Technical Report TR-192, Computer Science Center, University of Maryland.
ZACHARIASEN, W. H. (1967). *Acta Cryst.* **23**, 558–564.

Acta Cryst. (1974). A**30**, 757

Structure Factor Algebra in the Probabilistic Procedures for Phase Determination. III

BY C. GIACOVAZZO

Istituto di Mineralogia e Petrografia, Università di Bari, Italy

(*Received* 11 *March* 1974; *accepted* 19 *May* 1974)

An investigation has been carried out on the use of normalized, quasi-normalized and pseudo-normalized structure factors in the probabilistic procedures for phase assignment. A new statistical formula has been established for centrosymmetric space groups.

Introduction

Several ways of normalizing structure factors are used in the procedures for the solution of the phase problem by direct methods. In part I of this paper (Giacovazzo, 1974*a*) we have recalled the definitions of the normalized structure factor $E_{\mathbf{h}}$, the quasi-normalized structure factor $\mathscr{E}_{\mathbf{h}}$ and a pseudo-normalized structure factor $E'_{\mathbf{h}}$, this last advised by Karle & Karle (1966). $E_{\mathbf{h}}$ ensures always that the mean-square $\langle E_{\mathbf{h}}^2\rangle=1$ with the consequent simplicity in some distribution functions: the quasi-normalized structure factor $\mathscr{E}_{\mathbf{h}}$ warrants greater simplicity in the derivation of the algebraic relations.

In the automatic procedures for the calculation of crystal structure invariants (Hauptman, Fisher, Hancock & Norton, 1969), quasi-normalized structure factors are preferred: in actual symbolic-addition procedures or in the multisolution approach the use of E or E' is a personal decision. Giacovazzo (1974*a*, *b*) has shown that the statistical interactions among $E_{\mathbf{h}}, E_{\mathbf{k}}, E_{\mathbf{h}\pm\mathbf{k}}$ are not simple, but depend on the space groups and on the parity of the vectors $\mathbf{h},\mathbf{k},\mathbf{h}\pm\mathbf{k}$.

In fact, in centrosymmetric crystals the formula is

$$P_+(E_{\mathbf{h}})=\tfrac{1}{2}+\tfrac{1}{2}\tanh\left[\frac{E_{\mathbf{h}}}{N^{1/2}}\,W_{\mathbf{h},\mathbf{k}}E_{\mathbf{k}}E_{\mathbf{h}\pm\mathbf{k}}\right], \quad (1)$$

where

$$W_{\mathbf{h},\mathbf{k}}=\frac{1}{m}\,\frac{\langle\xi(\mathbf{h})\xi(\mathbf{k})\xi(\mathbf{h}\pm\mathbf{k})\rangle}{\sqrt{p_{\mathbf{h}}p_{\mathbf{k}}p_{\mathbf{h}\pm\mathbf{k}}}};$$

m is the order of the space group, ξ its trigonometric structure factor. If $E_{\mathbf{h}}$ is a non-centrosymmetric reflexion, we can write

$$P(\varphi_{\mathbf{h}})=\exp\{G_{\mathbf{h},\mathbf{k}}\cos(\varphi_{\mathbf{h}}-\varphi_{\mathbf{k}}-\varphi_{\mathbf{h}-\mathbf{k}})\}/[2\pi I_0(G_{\mathbf{h},\mathbf{k}})], \quad (2)$$

where

$$G_{\mathbf{h},\mathbf{k}}=\frac{1}{m}\,\frac{\langle\xi(-\mathbf{h})\xi(\mathbf{k})\xi(\mathbf{h}-\mathbf{k})\rangle}{\sqrt{p_{\mathbf{h}}p_{\mathbf{k}}p_{\mathbf{h}-\mathbf{k}}}}\,\frac{2}{\sqrt{N}}\,|E_{\mathbf{h}}E_{\mathbf{k}}E_{\mathbf{h}-\mathbf{k}}|\,.$$